Electronic Supplementary Material (ESI) for Chemical Communications.

Real Time Chemical Imaging of a Working Catalytic Membrane Reactor

A. Vamvakeros, S. D. M. Jacques*, V. Middelkoop*, M. Di Michiel, C. K. Egan, I. Z. Ismagilov, G. B.M. Vaughan, F. Gallucci, M. van Sint Annaland, P. R. Shearing, R. J. Cernik, A. M. Beale*

This section contains details regarding the preparation of catalyst and membranes and further details on the experimental setup (including two photographs of the XRD-CT experimental setup), a comment relating to an artefact present within this XRD-CT, normalised summed intensity changes (as a companion to Figure 2), XRD-CT data focusing on the BCFZ membrane, a diffraction pattern to illustrate the phase identification of $BaWO_4$, SEM-WDS data after the OCM experiments, micro-CT measurements before and after the OCM2 experiment and mass spectrometry data from the second OCM experiment.

Preparation of catalyst and membranes

2%Mn-1.6%Na-3.1%W/SiO_2 was prepared by a sequential incipient wetness impregnation method. Firstly, the SiO_2 support (Silica gel Davisil 646, ~ 250-500 μm) was impregnated by an aqueous solution of sodium tungstate dihydrate $Na_2WO_4{\cdot}2H_2O$ and sodium oxalate $Na_2C_2O_4$ salts taken in appropriate concentrations at a temperature of 80ºC. The Na-W/SiO_2 was dried at 120 ºC for 6 h and was then impregnated by an aqueous solution of manganese (II) acetate tetrahydrate $Mn(CH3COO)_2{\cdot}4H_2O$ salt taken in appropriate concentrations. The catalysts were then dried at 120°C for 6 h and calcined in air at 850 for 6 h with a heating rate of 2 ºC/min. The BCFZ membranes reported here have been manufactured using the spinning and phase inversion methods previously described.[1] The starting polymer suspension was prepared from cellulose acetate (CA, Mr ~52000, Fluka), dimethylsulphoxide (DMSO, Synthesis grade, Merck) and de-ionised water that were used as a phase-inversion polymer, solvent and non-solvent additive to the polymer solution, respectively.

Experimental Setup

XRD-CT measurements were made at station ID15A of ESRF using a 93 keV monochromatic beam focused to have a spot size of 20 x 20 μm. Diffraction patterns were collected by area detectors. The OCM1 experiment was performed with a Perkin Elmer XRD 1621 flat panel detector with a CsI conversion layer; the OCM2 experiment was done with a

Pilatus3 X CdTe 300K hybrid photon counting detector which uses Cadmium Telluride (CdTe) as the semiconducting direct conversion layer (Figure S1). The CT measurement was made with 130 translations over 180° in 1.8° steps covering a physical area of 2.6 x 2.6 mm. Reconstruction of these data yielded diffraction images with 130 x 130 pixels with 20 µm resolution. A catalytic membrane reactor suitable for the oxidative coupling of methane was prepared from a hollow-fibre BCFZ membrane (2.4 mm Ø and 180 µm wall thickness) packed with a 2%Mn-1.6%Na-3.1%W/SiO_2 catalyst supported between glass wool. The catalytic membrane reactor was glued on top of an alumina rod. The reactor cell (i.e. the CMR and the alumina rod) was inserted inside a quartz glass tube and a four-way Swagelok piece was used to allow the use of two different gas streams. Air was used at the outer side of the membrane and a mixture of CH_4 diluted in He at the inner side of the membrane.

The reactor was mounted into a gas delivery stub, itself mounted to a standard goniometer (to enable alignment). The goniometer was fixed to a rotation stage set upon a translation stage to facilitate the movements required for the CT measurement. Heating was achieved by virtue of two hot air blowers heating each side of the catalytic membrane reactor. XRD-CT measurements were made at nominal temperatures, ambient, 750, 850, 1000, 950, 850°C equating to actual temperatures (i.e. after temperature calibration) of ca. ambient, 675, 725, 775, 750, 725°C with a nominal ramp rate of 5 °C min^{-1}. During the in situ XRD-CT measurement, the outflow gasses were monitored by mass spectrometry using an Ecosys portable mass spectrometer. The mass spec line was inserted inside the membrane from the top. The experimental setup is shown in Figure S1.

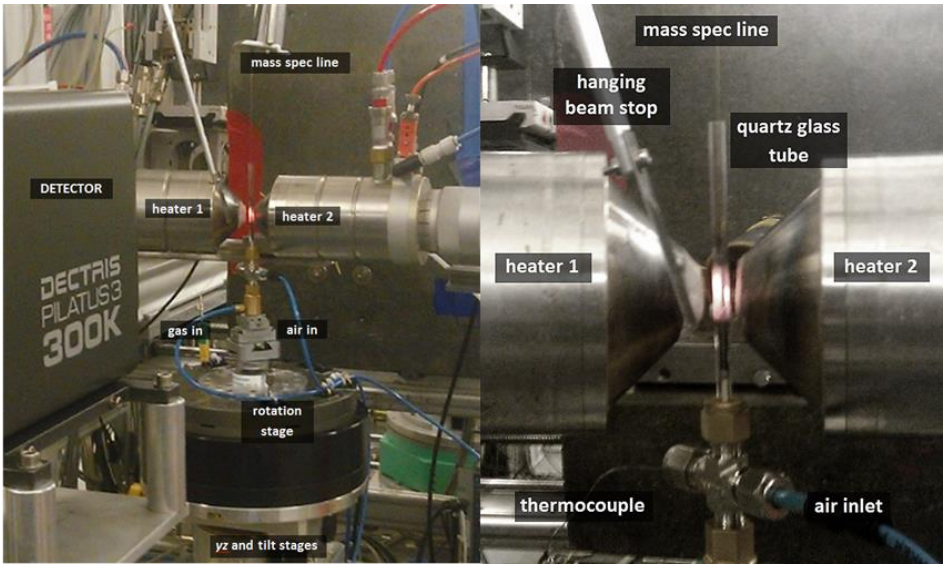

Figure S1. Photographs of the experimental setup used for XRD-CT at the ID15A beamline of the ESRF.

Comment 1: Absorption artefact

It should be the case that the diffraction observed within the voxel originates only from that part of the sample. Here though, it is important to point out that with these data (i.e. all that XRD-CT presented herein) contain an artefact because an adequate absorption correction was not included in the tomographic reconstruction algorithm. This artefact is apparent in the purple spectrum presented in Figure 1 (top right). This spectrum is from a selected position within the catalyst yet contains some strong peaks which are clearly seen to match the position of the membrane peaks visible in the yellow spectrum. Nevertheless, using our knowledge of the membrane from post analysis we are able to know the real bounds of our membrane and the artefact signal can be masked out.

BCFZ XRD-CT maps

The intensity distribution maps of the first four peaks of BCFZ from the OCM1 experiment are presented in Figure S3. These peaks correspond to the 100, 110, 111 and 200 BCFZ reflections respectively. It can be seen that no significant changes take place during the experiment regarding these intensity maps. However, there is a change for the maps that are generated from the intensity ratio of the 110 over the 200 reflection.

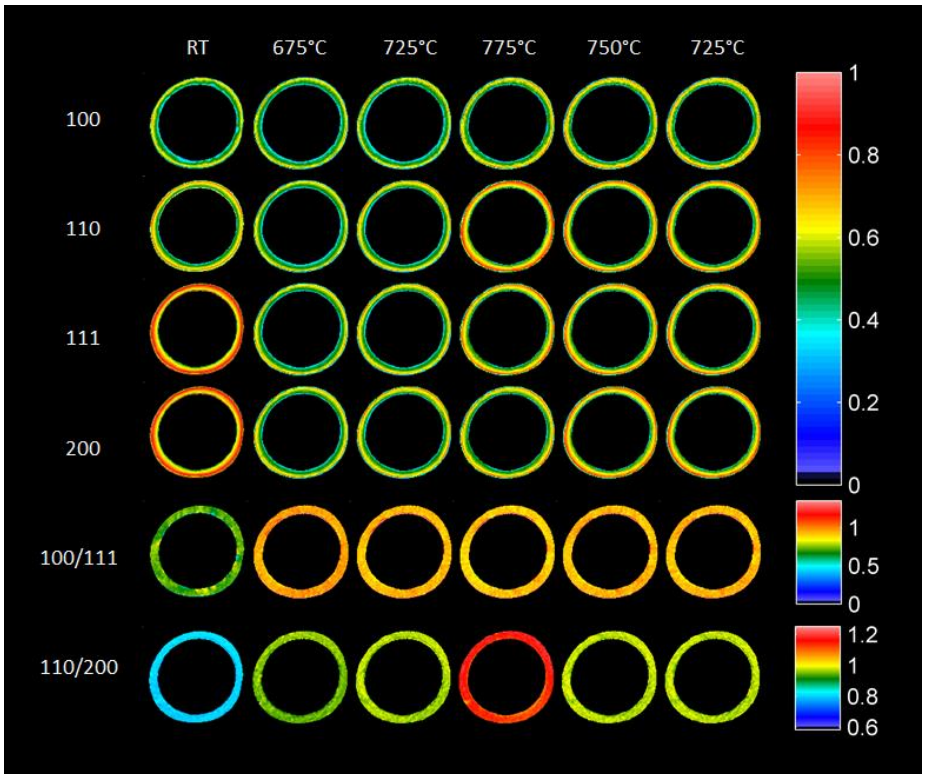

Figure S2. BCFZ normalized intensities for the 100, 110, 111 and 200 BCFZ reflections and reflection intensity ratios.

Phase identification of $BaWO_4$

Figure S5 shows a selected diffraction pattern at the membrane catalyst interface from XRD-CT slice at 725°C (OCM1 experiment) where the entire pattern can be described by the identified phases $BaWO_4$, cristobalite (the catalyst support), Mn_2O_3, tridymite (the catalyst support) and BCFZ (membrane material). These data were then fitted to obtain semi-quantitative data, thus phase maps showing distributions in space and time can be made. The phase maps were presented in Figure 2. The phase identification process using the ICSD database and the PDF-2013 database showed the same results (i.e. $BaWO_4$ was identified as the new phase that forms during the OCM experiments).

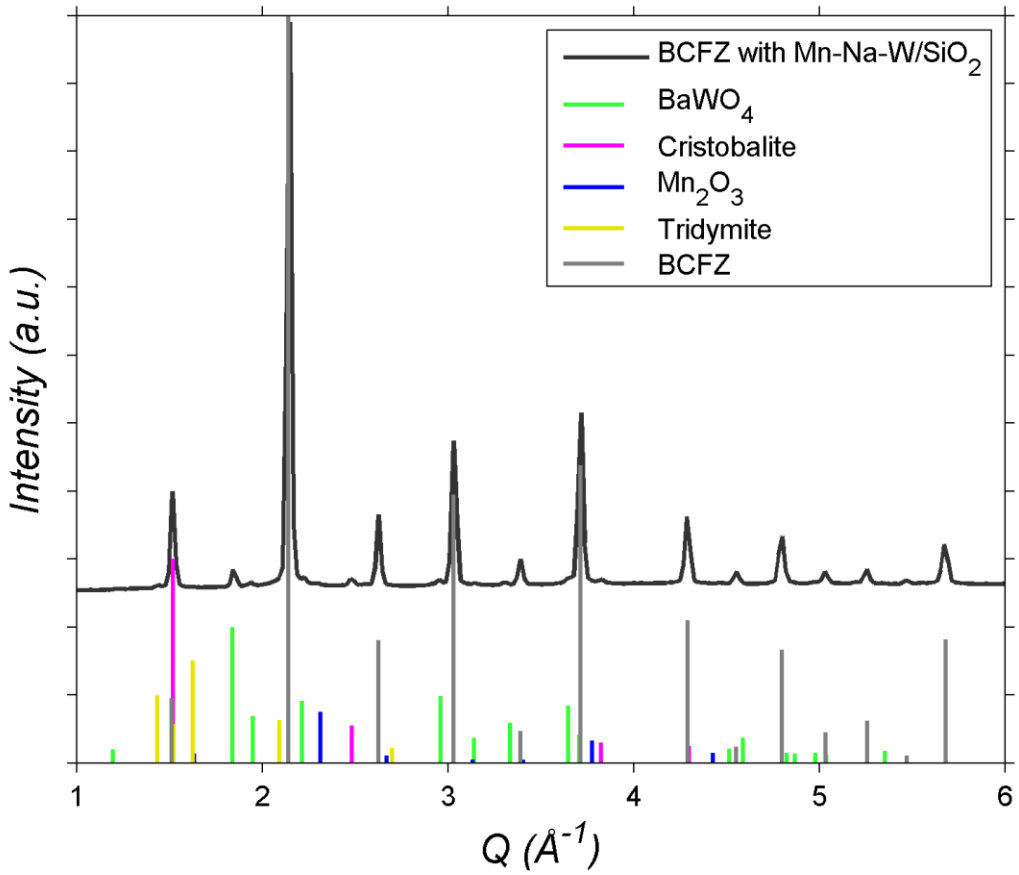

Figure S3. Phase identification of a summed diffraction pattern from pixels of interest (i.e. after applying a mask and taking into account only the pixels where the new $BaWO_4$ phase appears) at 725°C (OCM1 experiment). $BaWO_4$ (01-072-0746), β-cristobalite (01-076-0931), tridymite (01-073-0403) and Mn_2O_3 (01-076-0150) were identified using the PDF-2013 database. BCFZ is also shown although the crystal structure of BCFZ is not available in any crystallographic database. The result of peak indexing is a cubic unit cell (space group 221: Pm-3m).

Normalised summed intensity changes

Figure S2 shows the relative changes in cristobalite, tridymite, Mn_2O_3, $BaWO_4$ and the amorphous component during the OCM1 experiment is a companion to Figure 2 in the main text.

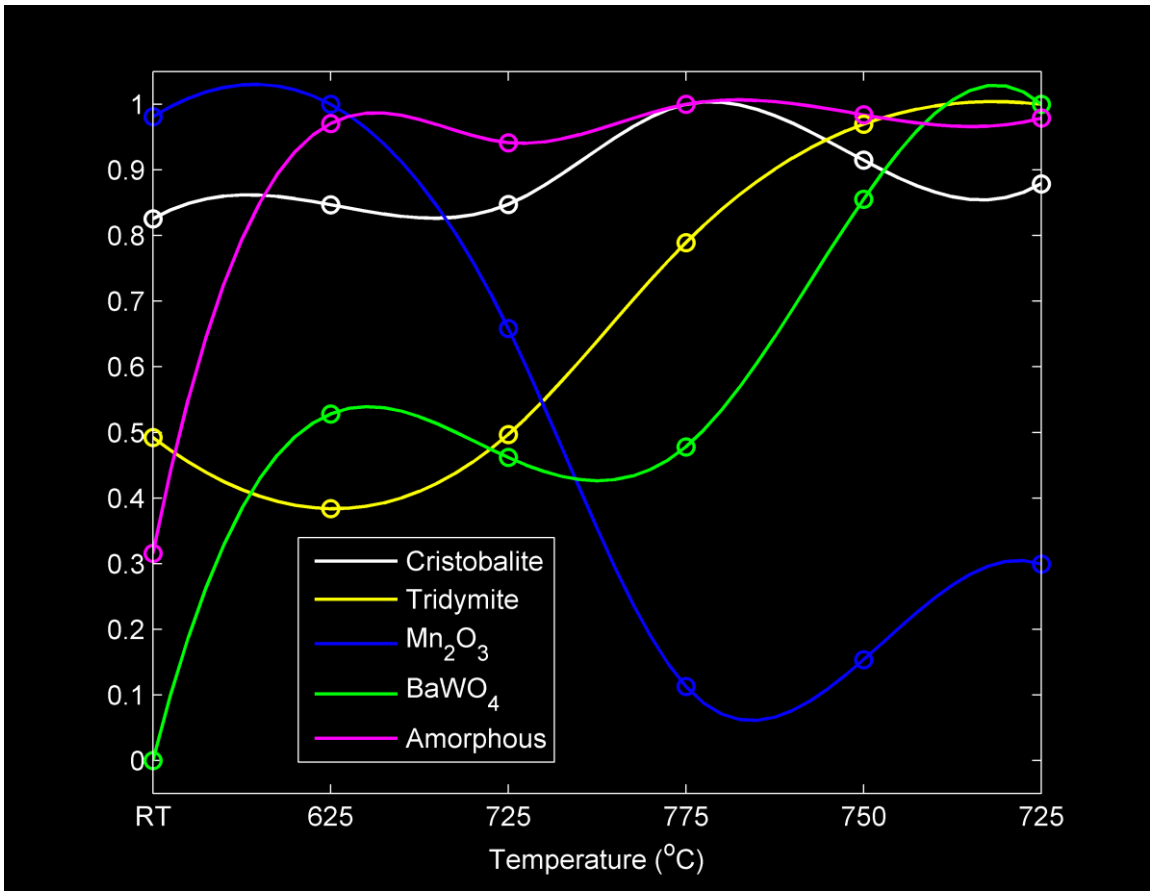

Figure S4. The relatives change in each component (normalized to the maximum value (ordinate) vs. temperature in ^{o}C (abscissa)) summed over the whole sample slice, as determined from the integrated intensities.

Mass Spectrometry measurements

The analysis of the gas products with mass spectrometry serves to illustrate that the integrated reactor system was captured in its active state. The mass spectrometry data from the OCM2 experiment are presented in Figure S7. Five regions are shown corresponding to air and different mixtures of CH_4 diluted in He (i.e. 5, 20, 50 and 100 vol. % CH_4 in He). The signal from mass 26, which corresponds to C_2H_2+ fractions, appears when the reaction mixture is used (i.e. 5% CH_4 in He). The intensity of this signal increases with increasing CH_4 concentration (i.e. 20, 50 and 100 vol. % CH_4 in He). This phenomenon is expected as it known from literature that the selectivity for C_2 molecules increases with increasing CH_4 concentration.[2] It also has to be noted that a signal from mass 41, which corresponds to C_3H_5+ fractions, appears when a mixture of 20% CH_4 in He is used and its intensity follows the same trend as the signal from mass 26. More importantly, the intensity of the signals corresponding to higher hydrocarbon molecules than CH_4 (i.e. C_2 and $_3$ fractions) did not decrease throughout the experiment, although the $BaWO_4$ phase was formed at the interphase between the catalyst particles and the BCFZ membrane.

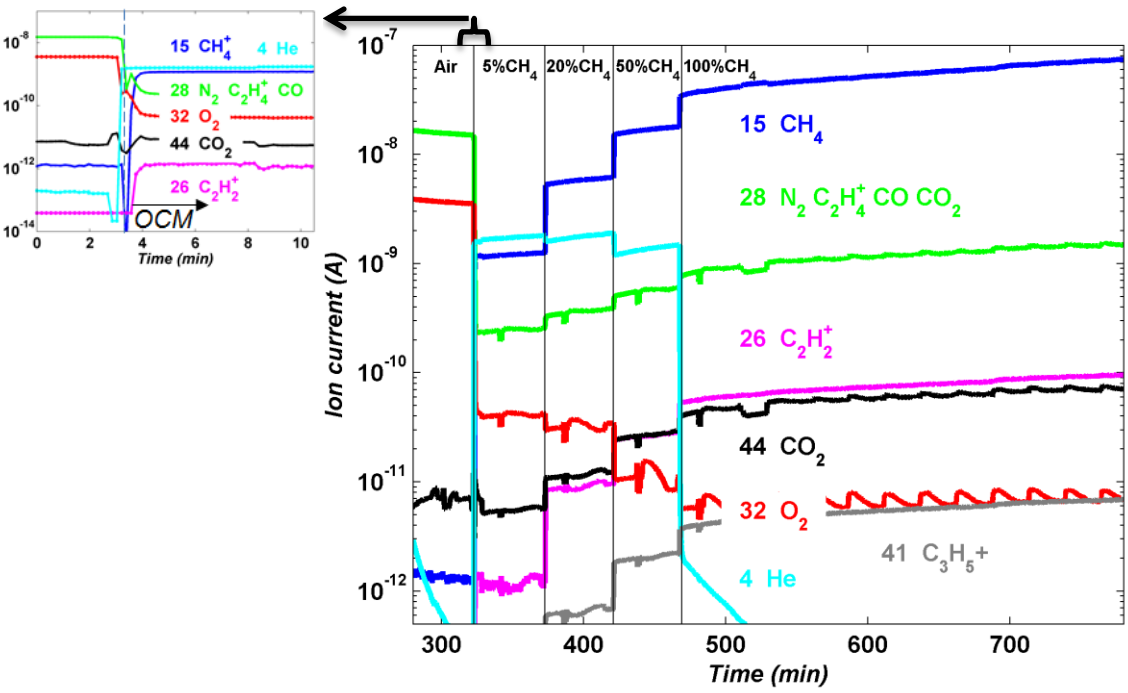

Figure S5. Mass spectrometry data corresponding to the following m/z ratios (possible species and respective line colour in parentheses): 4 (He - cyan), 15 (CH_4+ - blue), 28 (N_2, CO, C_2H_4+ - green), 32 (O_2 - red), 44 (CO_2 - black), 26 (C_2H_2+ - magenta) and 41 (C_3H_5+ - grey). Top left: Panel G of Figure 3 presented in the main article which shows a selected region of interest from the main figure of Figure S7. Note, for display purposes, the x axis for Figure 3 in the main text starts at 0 minutes (corresponding to 320 minutes on stream).

Micro-CT measurements

Micro-CT measurements from the OCM2 experiment are presented in Figure S6. Panels A and B show comparable slices from the reactor at room temperature prior to and after the OCM experiment. The red circle in panel A highlights a catalyst particle containing a high concentration of tungsten which seems to have diminished after OCM as indicated in the red circle in panel B. This is consistent with the observations of XRD-CT that a portion of the tungsten is migrating and depositing as $BaWO_4$ at the inner wall of the membrane. Hotspots of material are observed at the wall as can be seen in the reactor post OCM as is shown in panel C; example hotspots have been highlighted by the orange circle. A vertical slice from the same reconstruction is shown in panel D. The hotspots at the wall are clearly visible (again examples are highlighted in the orange circles).

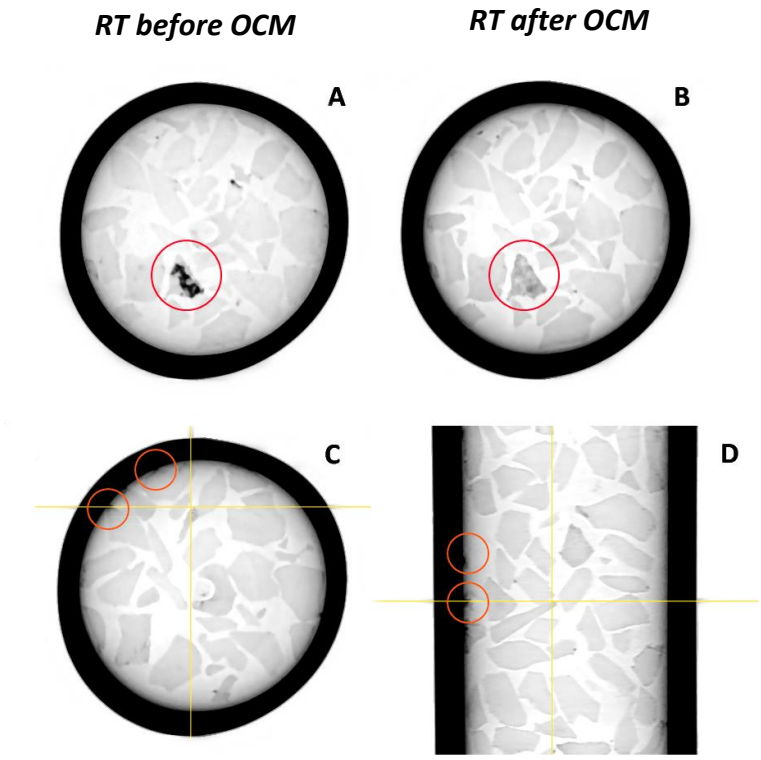

Figure S6. Reconstructed slices from micro-CT measurements before (Panel A and C) and after the second (Panel B and D) OCM experiment.

Microscopy and elemental analysis

In addition the cross-sectioned samples were imaged and analysed using Scanning Electron Microscopy coupled with Wavelength Dispersive X-ray Spectrometry (SEM-WDS). The morphological and elemental data were collected for the pre and post operation samples on a JEOL JXA8530F in-lens Schottky FEG-EPMA instrument (Field Emission Gun Electron Probe Micro-Analyser) fitted with five vertical crystal WDS detectors using an accelerating voltage of 15 keV and a beam current of 50 nA.

The results from the SEM/WDS measurements for the BCFZ with 2% Mn-1.6% Na-3.1% W/SiO_2 catalytic membrane reactor after the OCM experiment are shown in Figure S4. Two different scans were performed in the same area of the sample, taken at different magnification levels. The area of interest is highlighted (blue colour) at the top left section of Figure S4. The elemental maps of tungsten (W) clearly show that W has migrated from the catalyst particles to the inner side of the BCFZ membrane which supports the results from the XRD-CT scans (i.e. the formation of $BaWO_4$).

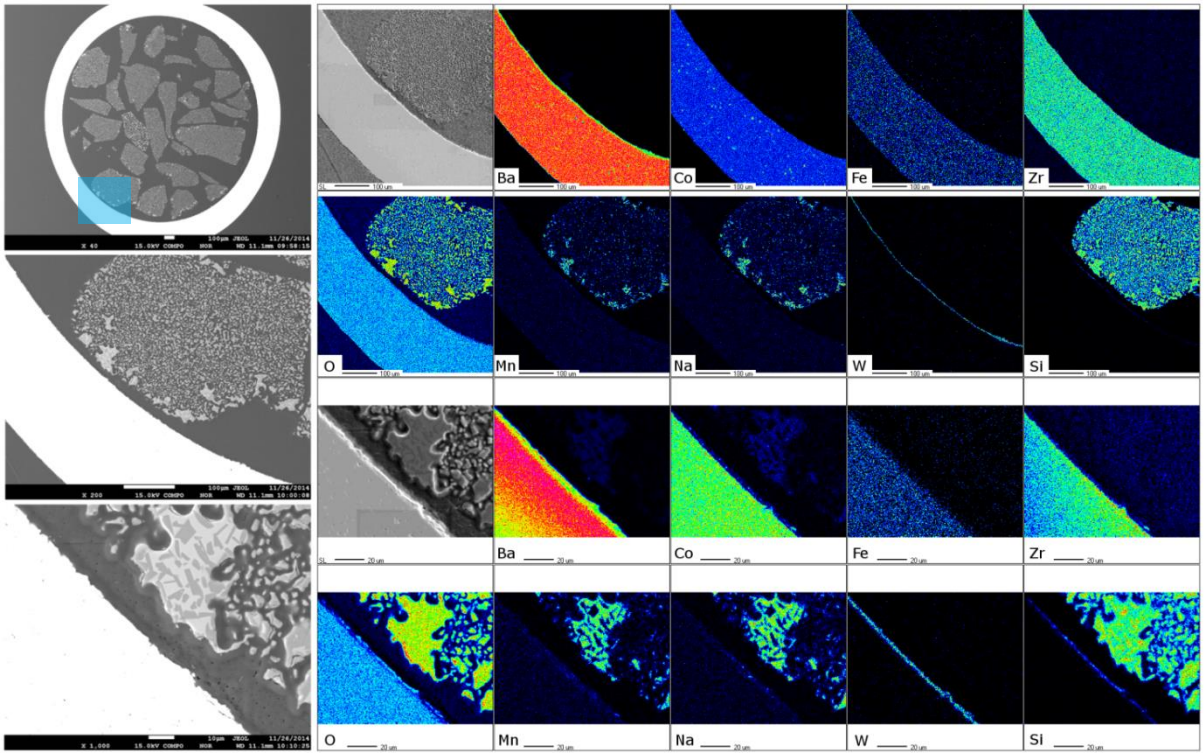

Figure S7. SEM images and WDS mapping of the cross section of BCFZ with 2% Mn-1.6% Na-3.1% W/SiO_2 CMR

Acknowledgements

The development of the catalysts and membranes for the catalytic membrane reactor used in this work is funded within the DEMCAMER project as part of the European Union Seventh Framework Programme (FP7/2007-2013) under grant agreement nº NMP3-LA-2011-262840. Note: "The present publications reflect only the authors' views and the Union is not liable for any use that may be made of the information contained therein." The authors would like to thank the European Synchrotron Radiation Source for beam time and CerPoTech AS for providing the ceramic powders. The authors would like to acknowledge support from the Hercules Foundation (project ZW09-09) for providing access to the FEG-EPMA at MTM-Catholic University of Leuven. Simon Jacques is supported under the EPSRC RCaH Impact Acceleration Fellowship. The authors Andrew M. Beale and Antonios Vamvakeros are also supported by the EPSRC funding. Paul R. Shearing acknowledges funding from the Royal Academy of Engineering.

Link to copies of raw data

Copies of the raw radially integrated XRD-CT data can be found at http://tiny.cc/C5CC03208C.

References

[1] a) J. Van Noyen, V. Middelkoop, C. Buysse, A. Kovalevsky, F. Snijkers, A. Buekenhoudt, S. Mullens, J. Luyten, J. Kretzschmar, S. Lenaerts, *Catal. Today* **2012**, *193*, 172-178; b) V. Middelkoop, H. Chen, B. Michielsen, M. Jacobs, G. Syvertsen-Wiig, M. Mertens, A. Buekenhoudt, F. Snijkers, *J. Membr. Sci.* **2014**, *468*, 250-258.

[2] O. Czuprat, T. Schiestel, H. Voss, J. Caro, *Ind. End. Chem. Res.* **2010**, *49*, 10230-10236.